Inorg. Chem. **2006**, *45*, 4055–4064

Construction of [(η^5-C_5Me_5)WS_3Cu_3]-Based Supramolecular Compounds from Preformed Incomplete Cubane-Like Clusters [PPh_4][(η^5-C_5Me_5)WS_3(CuX)$_3$] (X = CN, Br)

Qing-Feng Xu,[†] Jin-Xiang Chen,[†] Wen-Hua Zhang,[†] Zhi-Gang Ren,[†] Hong-Xi Li,[†] Yong Zhang,[†] and Jian-Ping Lang*[,†,‡]

Key Laboratory of Organic Synthesis of Jiangsu Province, School of Chemistry and Chemical Engineering, Suzhou University, 180 GongYeYuanQuHengYiLu, Suzhou 215123, Jiangsu, P. R. China, and State Key Laboratory of Coordination Chemistry, Nanjing University, Nanjing 210093, Jiangsu, P. R. China

Received January 19, 2006

Approaches to the assembly of (η^5-C_5Me_5)WS_3Cu_3-based supramolecular compounds from two preformed incomplete cubane-like clusters [PPh_4][(η^5-C_5Me_5)WS_3(CuX)$_3$] (X = CN, **1a**; X = Br, **1b**) have been investigated. Treatment of **1a** with LiBr/1,4-pyrazine (1,4-pyz), pyridine (py), LiCl/py, or 4,4′-bipyridine (4,4′-bipy) and treatment of **1b** with 4,4′-bipy gave rise to a new set of W/Cu/S cluster-based compounds, [Li{((η^5-C_5Me_5)WS_3Cu_3(μ_3-Br))$_2$(μ-CN)$_3$}·C_6H_6]$_\infty$ (**2**), [(η^5-C_5Me_5)WS_3Cu_3(μ-CN)$_2$(py)]$_\infty$ (**3**), {[PPh_4][(η^5-C_5Me_5)WS_3Cu_3(μ_3-Cl)(μ-CN)(CN)]·py}$_\infty$ (**4**), [PPh_4]$_2$-[(η^5-C_5Me_5)WS_3Cu_3(CN)$_2$]$_2$(μ-CN)$_2$·(4,4′-bipy) (**5**), and {[(η^5-C_5Me_5)WS_3Cu_3Br(μ-Br)(4,4′-bipy)]·Et_2O}$_\infty$ (**6**). The structures of **2**–**6** have been characterized by elemental analysis, IR spectra, and single-crystal X-ray crystallography. Compound **2** displays a 1D ladder-shaped chain structure built of squarelike {[(η^5-C_5Me_5)WS_3Cu_3(μ_3-Br)(μ-CN)]$_4$}-(μ-CN)$_2^{2-}$ anions via two pairs of Cu–μ-CN–Cu bridges. Compound **3** consists of a single 3D diamondlike network in which each (η^5-C_5Me_5)WS_3Cu_3 unit, serving as a tetrahedral node, interconnects with four other nearby units through Cu–μ-CN–Cu bridges. Compound **4** contains a 1D zigzag chain array made of cubane-like [(η^5-C_5Me_5)WS_3-Cu_3(μ_3-Cl)(μ-CN)(CN)]$^-$ anions linked by a couple of Cu–μ-CN–Cu bridges. Compound **5** contains a dimeric structure in which the two incomplete cubane-like [(η^5-C_5Me_5)WS_3(CuCN)$_2$(μ-CN)]$^-$ anions are strongly held together via a pair of Cu–μ-CN–Cu bridges. Compound **6** contains a 2D brick-wall layer structure in which dimers of [(η^5-C_5-Me_5)WS_3Cu_3Br(4,4′-bipy)]$_2$ are interconnected via four Cu–μ-Br–Cu bridges. The successful construction of (η^5-C_5Me_5)WS_3Cu_3-based supramolecular compounds **2**–**6** from the geometry-fixed clusters **1a** and **1b** may expand the scope of the rational design and construction of cluster-based supramolecular assemblies.

Introduction

Rational design and assembly of supramolecular compounds from preformed complexes remain a great challenge to chemists in the world.[1] Transition-metal clusters, by virtue of their well-defined structures and unique properties, present themselves as an attractive class of structural and functional building blocks in supramolecular chemistry.[1−7] So far, several interesting approaches have been reported for the generation of new cluster-based supramolecular arrays. For example, some metal−metal bonded dimeric clusters [M_2-(DArF)$_2$(MeCN)$_4$]$^{2+}$ (M = Mo, Rh) were adopted as building

* To whom correspondence should be addressed. E-mail: jplang@suda.edu.cn.
† Suzhou University.
‡ Nanjing University.

(1) (a) Lehn, J. M., *Supramolecular Chemistry and Perspectives*; *VCH*: Weinheim, Germany, 1995; p 139. (b) Stang, P. J.; Olenyuk, B. *Acc. Chem. Res.* **1997**, *30*, 502. (c) Robson, R.; Hoskins, B. F. *J. Am. Chem. Soc.* **1990**, *112*, 1546. (d) Blake, A. J.; Champness, N. R.; Khlobystov, A. N.; Parsons, S.; Schröder, M. *Angew. Chem., Int. Ed.* **2000**, *39*, 2317.

(2) (a) Rosi, N. L.; Eckert, J.; Eddaoudi, M.; Vadak, D. T.; Kim, J.; O'Keeffe, M.; Yaghi, O. M. *Science* **2003**, *300*, 1127. (b) Eddaoudi, M.; Moler, D. B.; Li, H. L.; Chen, B.; Reineke, T. M.; O'Keeffe, M.; Yaghi, O. M. *Acc. Chem. Res.* **2001**, *34*, 319. (c) Yaghi, O. M.; Li, H. L.; Davis, C.; Richardson, D.; Groy, T. L. *Acc. Chem. Res.* **1998**, *31*, 474. (d) Vodak, D. T.; Braun, M. E.; Kim, J.; Eddaoudi, M.; Yaghi, O. M. *Chem. Commun.* **2001**, 2534.

(3) (a) Cotton, F. A.; Lin, C.; Murillo, C. A. *Acc. Chem. Res.* **2001**, *34*, 750. (b) Cotton, F. A.; Dikarev, E. V.; Petrukhina, M. A.; Schmitz, M.; Stang, P. J. *Inorg. Chem.* **2002**, *41*, 2903. (c) Cotton, F. A.; Lin, C.; Murillo, C. A. *Inorg. Chem.* **2001**, *40*, 5886. (d) Cotton, F. A.; Lin C.; Murillo, C. A. *Chem. Commun.* **2001**, 11.

10.1021/ic060115p CCC: $33.50
Published on Web 04/21/2006

blocks for generating a new family of M_2-based supramolecular compounds.[3] Octahedral hexarhenium chalcogenide clusters were utilized to create a series of $[Re_6Q_8]$ (Q = S, Se, Te)-based supramolecular arrays, some of which may have interesting photophysical properties.[4] A series of chiral cluster-based polymers were produced from the interlinking of linear $\{[Cu(threo\text{-}tab)]^{2+}\}_\infty$ (threo-tab = 1,2*S*,3*S*,4-butanetetramine) strands with $[Re_4Te_4(CN)_{12}]^{4-}$ and $[Re_6Q_8(CN)_6]^{4-}$ (Q = Te, Se, S) in alkaline aqueous solution.[5d] However, the development in this type of study has slowed because of the limited suitable cluster precursors and the difficulty in isolating the resulting products.

On the other hand, in the past decades, synthesis of new heteronuclear clusters from reactions of thiomolybdate and thiotungstate with various metals have attracted much attention because of their interesting chemistry and their relevance to biological systems, industrial catalysis, and photonic materials.[8−17] Recently, we have been interested in the assembly of cluster-based supramolecular compounds using preformed Mo(W)/Cu/S clusters in the pursuit of new cluster chemistry and new chemical and/or physical properties.[17] We communicated the assembly of a W/Cu/S cluster-based supramolecular cube, $[((\eta^5\text{-}C_5Me_5)WS_3Cu_3)_8Cl_8(CN)_{12}Li_4]$, from reactions of a preformed incomplete cubane-like cluster, $[PPh_4][(\eta^5\text{-}C_5Me_5)WS_3(CuCN)_3]$ (**1a**), with LiCl and 1,4-pyrazine (1,4-pyz).[17b] This result prompted us to consider **1a** and its bromide analogue, $[PPh_4][(\eta^5\text{-}C_5Me_5)WS_3(CuBr)_3]$ (**1b**), as useful cluster precursors for generating other topological structures.

As shown in Scheme 1, compound **1a** or **1b** may be viewed as having an incomplete cubane-like $[(\eta^5\text{-}C_5Me_5)WS_3Cu_3]$ core structure in which three Cu atoms have a typical trigonal planar coordination geometry and three terminal cyanides (or bromides) extend in directions that are approximately perpendicular to each other. The three copper centers in the cluster core of **1a** or **1b** may have up to six coordination sites available if their coordination geometries are turned into a tetrahedral one. Topologically, the cluster cores in **1a** and **1b** are anticipated to serve as multiconnecting nodes (nodes a−f in Scheme 1) for the assembly of cluster-based supramolecular frameworks. For example, if halide X from LiX is introduced to cap the void of the incomplete cubane-like core of **1a**, it may form a cubane-like $[(\eta^5\text{-}C_5Me_5)WS_3Cu_3X(CN)_3]^-$ species. Therefore, it may act as a two-connecting (d) or three-connecting node (a or b), forming a 1D zigzag chain, a supramolecular cube, or a 1D ladder-shaped chain. If LiX is absent, the six possible coordination sites of **1a** or **1b** may make the assembly process more complicated. When the $[(\eta^5\text{-}C_5Me_5)WS_3Cu_3]$ core acts as a four-connecting node (c), mono-connecting (e) or three-connecting node (f), it may form a unique 3D diamondlike network, a dimer structure, or a 2D brick-wall layer network.

For the formation of the above topological structures to be achieved, some nitrogen donor ligands should be adopted to remove part of the cyanides or bromides of **1a** or **1b**, and the remaining species would be connected by the ditopic linkers existing in the same system.[17b] Then what nitrogen donor ligands could be used for this purpose? With that question in mind, we attempted reactions of **1a** or **1b** with 1,4-pyrazine (1,4-pyz), pyridine (py), or 4,4′-bipyridine (4,4′-bipy), and successfully isolated a set of five unique $[(\eta^5\text{-}C_5Me_5)WS_3Cu_3]$-based assemblies: $[Li\{((\eta^5\text{-}C_5Me_5)WS_3Cu_3(\mu_3\text{-}Br))_2(\mu\text{-}CN)_3\}\cdot C_6H_6]_\infty$ (**2**), $[(\eta^5\text{-}C_5Me_5)WS_3Cu_3(\mu\text{-}CN)_2(py)]_\infty$ (**3**), $\{[PPh_4][(\eta^5\text{-}C_5Me_5)WS_3Cu_3(\mu_3\text{-}Cl)(\mu\text{-}CN)(CN)]\cdot py\}_\infty$ (**4**), $[PPh_4]_2[(\eta^5\text{-}C_5Me_5)WS_3Cu_3(CN)_2]_2(\mu\text{-}CN)_2\cdot(4,4'\text{-bipy})$ (**5**), and $\{[(\eta^5\text{-}C_5Me_5)WS_3Cu_3Br(\mu\text{-}Br)(4,4'\text{-bipy})]\cdot Et_2O\}_\infty$ (**6**). Herein, we report the isolation and structural characterization of **2**−**6**, which represents our initial ambition toward the rational design and construction of cluster-based supramolecular arrays from the preformed W/Cu/S clusters.

Experimental Section

General Procedures. Compounds $[PPh_4][(\eta^5\text{-}C_5Me_5)WS_3(CuX)_3]$ (**1a**, X = CN; **1b**, X = Br) were prepared as reported

(4) (a) Roland, B. K.; Carter, C.; Zheng, Z. P. *J. Am. Chem. Soc*. **2002**, *124*, 6234. (b) Zheng, Z. P. *Chem. Commun.* **2001**, 2521. (c) Roland, B. K.; Selby, H. D.; Carducci, M. D.; Zheng, Z. P. *J. Am. Chem. Soc*. **2002**, *124*, 3222. (d) Selby, H. D.; Roland, B. K.; Zheng, Z. P. *Acc. Chem. Res.* **2003**, *36*, 933.

(5) (a) Jin, S.; DiSalvo, F. J. *Chem. Mater.* **2002**, *14*, 3448. (b) Bain, R. L.; Shriver, D. F.; Ellis, D. E. *Inorg. Chim. Acta* **2001**, *325*, 171. (c) Naumov, N. G.; Cordier, S.; Perrin, C. *Angew. Chem., Int. Ed.* **2002**, *41*, 3002. (d) Mironov, Y. V.; Naumov, N. G.; Brylev, K. A.; Efremova, Q. A.; Fedorov, V. E.; Hegetschweiler, K. *Angew. Chem., Int. Ed*. **2004**, *43*, 1297.

(6) (a) Seidel, S. R.; Stang, P. J. *Acc. Chem. Res*. **2002**, *35*, 972. (b) Long, J. R.; McCarty, L. S.; Holm, R. H. *J. Am. Chem.* Soc. **1996**, *118*, 4603. (c) Beauvais, L. G.; Shores, M. P.; Long, J. R. *J. Am. Chem. Soc*. **2000**, *122*, 2763. (d) Bennett, M. V.; Beauvais, L. G.; Shores, M. P.; Long, J. R. *J. Am. Chem. Soc.* **2001**, *123*, 8022. (e) Tulsky, E. G.; Crawford, N. R. M.; Baudron, S. A.; Batail, P.; Long, J. R. *J. Am. Chem. Soc*. **2003**, *125*, 15543. (f) Yan, B. B.; Zhou, H. J.; Lachgar, A. *Inorg. Chem.* **2003**, *42*, 8818. (g) Yan, Z. H.; Day, C. S.; Lachgar, A. *Inorg. Chem.* **2005**, *44*, 4499.

(7) (a) Abrahams, B. F.; Egan, S. J.; Robson, R. *J. Am. Chem. Soc*. **1999**, *121*, 3535. (b) Abrahams, B. F.; Haywood, M. G.; Robson, R. *Chem. Commun.* **2004**, 938.

(8) (a) Müller, A.; Diemann, E.; Jostes, R.; Bögge, H. *Angew. Chem., Int. Ed*. **1981**, *20*, 934. (b) Müller, A.; Bögge, H.; Schimanski, U.; Penk, M.; Nieradzik, K.; Dartmann, M.; Krickemeyer, E.; Schimanski, J.; Römer, C.; Römer, M.; Dornfeld, H.; Wienböker, U.; Hellmann, W. *Monatsh. Chem.* **1989**, *120*, 367. (c) Jeannin, Y.; Séheresse, F.; Bernes, S.; Robert, F. *Inorg. Chim. Acta* **1992**, *198*−*200*, 493.

(9) (a) Adams, R. D., Cotton, F. A., Eds. *Catalysis by Di- and Polynuclear Metal Cluster Complexes*; Wiley-VCH: New York, 1998. (b) Hernandez-Molina, R.; Sykes, A. G. *J. Chem. Soc., Dalton Trans.* **1999**, 3137. (c) Hidai, M.; Kuwata, S.; Mizobe, Y. *Acc. Chem. Res.* **2000**, *33*, 46.

(10) (a) Wu, X. T.; Chen, P. C.; Du, S. W.; Zhu, N. Y.; Lu, J. X. *J. Cluster Sci*. **1994**, *5*, 265. (b) Wu, D. X.; Hong, M. C.; Cao, R.; Liu, H. Q. *Inorg. Chem*. **1996**, *35*, 1080.

(11) (a) Ansari, M. A.; Ibers, J. A. *Coord. Chem. Rev*. **1990**, *100*, 223. (b) Hou, H. W.; Xin, X. Q.; Shi, S. *Coord. Chem. Rev*. **1996**, *153*, 25.

(12) Lang, J. P.; Ji, S. J.; Xu, Q. F.; Shen, Q.; Tatsumi, K. *Coord. Chem. Rev*. **2003**, *241*, 47.

(13) George, G. N.; Pickering, I. J.; Yu, E. Y.; Prince, R. C.; Bursakov, S. A.; Gavel, O. Y.; Moura, I.; Moura, J. J. G. *J. Am. Chem. Soc*. **2000**, *122*, 8321.

(14) Shi, S.; Ji, W.; Tang, S. H.; Lang, J. P.; Xin, X. Q. *J. Am. Chem. Soc*. **1994**, *116*, 3615.

(15) Shi, S. In *Optoelectronic Properties of Inorganic Compounds*; Roundhill, D. M., Fackler, J. P., Jr., Eds.; Plenum Press: New York, 1998; p 55.

(16) Che, C. M.; Xia, B. H.; Huang, J. S.; Chan, C. K.; Zhou, Z. Y.; Cheung, K. K. *Chem.*−*Eur. J*. **2001**, *7*, 3998.

(17) (a) Lang, J. P.; Kawaguchi, H.; Tatsumi, K. *Chem. Commun.* **1999**, 2315. (b) Lang, J. P.; Xu, Q. F.; Chen, Z. N.; Abrahams, B. F. *J. Am. Chem. Soc.* **2003**, *125*, 12682. (c) Lang, J. P.; Xu, Q. F.; Yuan, R. X.; Abrahams, B. F. *Angew. Chem., Int. Ed*. **2004**, *43*, 4741. (d) Lang, J. P.; Jiao, C. M.; Qiao, S. B.; Zhang, W. H.; Abrahams, B. F. *Inorg. Chem*. **2005**, *44*, 2664.

Scheme 1

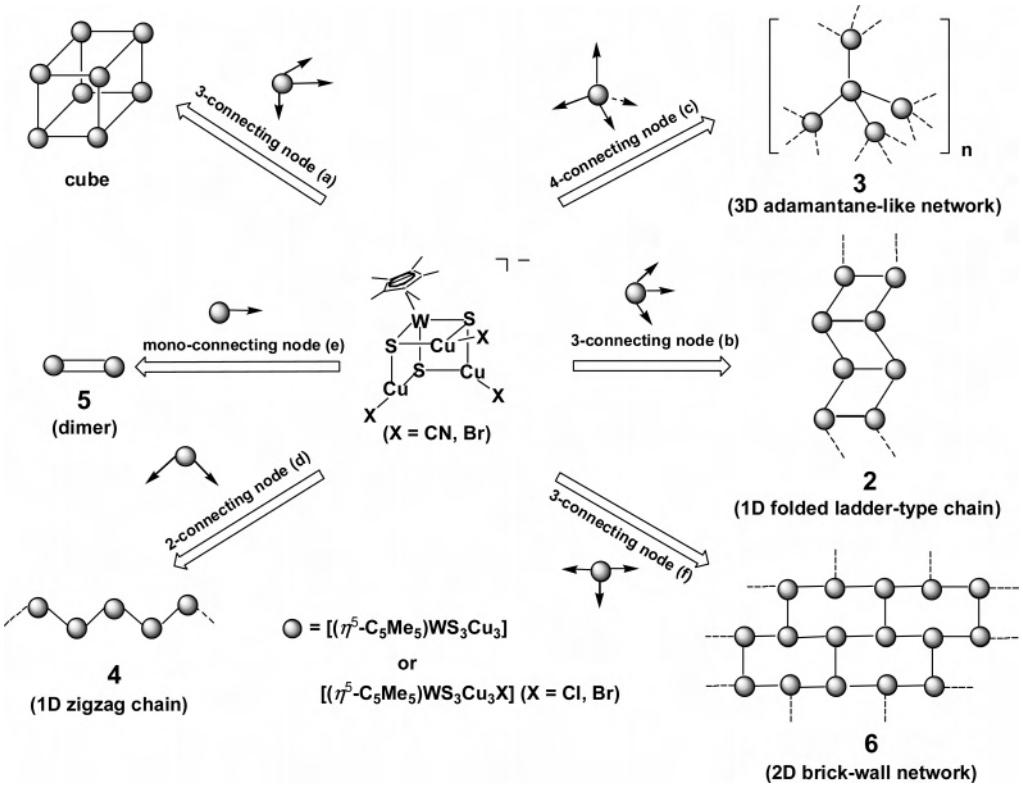

previously.[17b,18a] Other chemicals were obtained from commercial sources and used as received. All solvents were predried over activated molecular sieves and refluxed over the appropriate drying agents under argon. The IR spectra were recorded on a Nicolet MagNa-IR500 FT-IR spectrometer (4000−400 cm^{-1}). The elemental analyses for C, H, and N were performed on a Carlo−Erba CHNO-S microanalyzer.

[Li{(η^5-C_5Me_5)WS_3Cu_3(μ_3-Br))$_2$(μ-CN)$_3$}·C_6H_6]$_\infty$ (2). To a solution of **1a** (52 mg, 0.05 mmol) in 5.0 mL of MeCN were added LiBr (2.2 mg, 0.025 mmol) and 1,4-pyz (8 mg, 0.1 mmol). The mixture was stirred for 20 min and filtered. Benzene (2 mL) and diethyl ether (8 mL) were carefully layered onto the surface of the filtrate in a glass tube (length = 25 cm, ϕ = 0.6 cm), which was then capped with a rubber septa and tightly sealed with Parafilm. When the glass tube was left to stand at room temperature for two weeks, red plates of **2** were formed, coupled with a large amount of red crystals; the crystals were collected by filtration, washed thoroughly with 1:4 v/v MeCN:Et_2O, and dried in vacuo. Yield: 9 mg (25%). Anal. Calcd. for $C_{23}H_{30}Br_2Cu_6LiN_3S_6W_2$: C, 18.97; H, 2.08; N, 2.89. Found: C, 19.22; H, 2.07; N, 2.96. IR (KBr disk): 2137 (m), 1481 (s), 1377 (s), 1095 (s), 1026 (s), 528 (m), 439 (m) cm^{-1}.

[(η^5-C_5Me_5)WS_3Cu_3(μ-CN)$_2$(py)]$_\infty$ (3). Compound **1a** (52 mg, 0.05 mmol) was dissolved into 2.0 mL of pyridine. The resulting red solution was briefly stirred at room temperature and filtered. The filtrate was then transferred into a zigzag glass tube, and 5.0 mL of methanol was carefully layered onto the surface of the filtrate. This was followed by the slow addition of 10 mL of diethyl ether. The glass tube was capped with rubber septa and was tightly sealed with Parafilm. When the glass tube was left to stand at room temperature for one week, red prisms of **3** were formed, coupled with some orange-red crystals; the crystals were collected by filtration, washed thoroughly with 1:4 v/v MeCN/Et_2O, and dried in vacuo. Yield: 26 mg (70%). Anal. Calcd. for $C_{17}H_{20}Cu_3N_3S_3W$: C, 27.70; H, 2.76; N, 5.70. Found: C, 27.98; H, 3.21; N, 5.76. IR (KBr disk): 2152 (m), 1628 (m), 1385 (s), 469 (w), 424 (w) cm^{-1}.

{[PPh_4][(η^5-C_5Me_5)WS_3Cu_3(μ_3-Cl)(μ-CN)(CN)]·py**}$_\infty$ (4).** To a MeCN solution containing **1a** (52 mg, 0.05 mmol) and LiCl (2 mg, 0.05 mmol) was added 2.0 mL of pyridine. The mixture was stirred for 20 min and filtered. A workup similar to that used for the isolation of **3** afforded red platelets of **4**, which were collected by filtration, washed with Et_2O, and dried in vacuo. Yield: 36 mg (65%). Anal. Calcd. for $C_{41}H_{40}ClCu_3N_3PS_3W$: C, 44.29; H, 3.63; N, 3.78. Found: C, 44.36; H, 3.60; N, 3.76. IR (KBr disk): 2160 (m), 2120 (w), 1483 (m), 1436 (s), 1376 (m), 1108 (vs), 996 (m), 753 (m), 724 (vs), 690 (vs), 527 (vs), 445 (w), 430 (w) cm^{-1}.

[PPh_4]$_2$[(η^5-C_5Me_5)WS_3Cu_3(CN)$_2$]$_2$(μ-CN)$_2$·(4,4′-bipy) (5). To a red solution of **1a** (52 mg, 0.05 mmol) in MeCN (10 mL) was added 4,4′-bipy (22 mg, 0.10 mmol). The mixture was briefly stirred at room temperature for 1 min, and some orange-red materials gradually precipitated, which were centrifuged to give a red solution. A workup similar to that used for the isolation of **3** gave rise to red platelets of **5** mixed with a large amount of red-orange powder. The crystals were separated by filtration, washed thoroughly with MeOH and Et_2O, and dried in vacuo. Yield: 30 mg (41%). Anal. Calcd. for $C_{84}H_{78}Cu_6N_8P_2S_6W_2$: C, 45.97; H, 3.59; N, 5.11. Found: C, 45.89; H, 3.67; N, 5.30. IR (KBr disk): 2126 (m), 1585 (m), 1439 (m), 1439 (m), 1381 (s), 1262 (m), 1107 (s), 1026 (m), 806 (m), 725 (s), 690 (m), 528 (s), 428 (s) cm^{-1}.

{[(η^5-C_5Me_5)WS_3Cu_3Br(μ-Br)(4,4′-bipy)]·Et_2O}$_\infty$ (6). Treatment of **1b** (38 mg, 0.016 mmol) in DMF (3 mL) with 4,4′-bipy (11 mg, 0.067 mmol) gave rise to a homogeneous solution, which was stirred for 5 min and filtered. A workup similar to that used for the isolation of **3** gave rise to very thin red plates of **6**, which were collected by filtration, washed with Et_2O, and dried in vacuo.

(18) (a) Lang, J. P.; Kawaguchi, H.; Ohnishi, S.; Tatsumi, K. *J. Chem. Soc, Chem. Commun.* **1997**, 405. (b) Lang, J. P.; Kawaguchi, H.; Ohnishi, S.; Tatsumi, K. *Inorg. Chim. Acta* **1998**, *283*, 136.

Table 1. Summary of Crystallographic Data for **2**−**6**

	2	**3**	**4**	**5**	**6**
formula	$C_{29}H_{36}Br_2Cu_6LiN_3S_6W_2$	$C_{17}H_{20}Cu_3N_3S_3W$	$C_{41}H_{40}ClCu_3N_3PS_3W$	$C_{84}H_{70}Cu_6N_8P_2S_6W_2$	$C_{24}H_{23}Br_2Cu_3N_2OS_3W$
fw	1534.67	737.01	1111.83	2194.72	985.91
cryst syst	orthorhombic	orthorhombic	monoclinic	triclinic	orthorhombic
space group	*Cmcm*	$P2_12_12_1$	$P2_1/c$	$P\bar{1}$	*Pbcn*
a (Å)	26.854(5)	8.7069(8)	21.532(4)	9.964(2)	19.529(4)
b (Å)	14.287(3)	15.6615(17)	14.132(3)	14.490(3)	14.994(3)
c (Å)	14.697(3)	16.1002(17)	14.589(3)	16.071(3)	22.238(4)
α (deg)				78.13(3)	
β (deg)	104.30(3)			83.88(3)	
γ (deg)				77.82(3)	
V (Å^3)	5639(2)	2195.5(4)	4302.7(16)	2214.7(8)	6152 (2)
Z	4	4	4	1	8
D_c (g cm^{-3})	1.808	2.230	1.717	1.646	2.011
μ (mm^{-1})	7.937	8.381	4.405	4.220	8.120
no. of reflns collected	11451	18363	41319	22896	59231
no. of unique reflns	2566	3872	7856	8906	5947
no. of observed reflns	1792 ($I > 2.00\sigma(I)$)	3826 ($I > 2.00\sigma(I)$)	6081 ($I > 2.00\sigma(I)$)	8168($I > 2.00\sigma(I)$)	5061($I > 2.00\sigma(I)$)
params	126	250	442	457	301
R[a]	0.1027	0.0356	0.1028	0.0633	0.1237
wR[b]	0.2172	0.0693	0.2141	0.1686	0.2353
GOF[c]	1.216	1.174	1.224	1.138	1.292
largest residual peaks and holes (e Å^{-3})	1.412, −1.591	1.015, −0.974	1.406, −1.365	1.430, −1.669	1.760, −1.700

[a] $R = \sum||F_o| - |F_c||/\sum|F_o|$. [b] $wR = \{w\sum(F_o^2 - F_c^2)^2/\sum w(F_o^2)^2\}^{1/2}$. [c] $GOF = \{\sum w(F_o^2 - F_c^2)^2/(n-p)\}^{1/2}$, where *n* is the number of reflections and *p* is the number of parameters.

Yield: 18 mg (60%). Anal. Calcd. for $C_{20}H_{23}Br_2Cu_3N_2S_3W$: C, 26.06; H, 2.51; N, 3.04. Found: C, 26.22; H, 2.60; N, 3.18. IR (KBr disk): 1667 (m), 1604 (s), 1532 (m), 1485 (s), 1412 (s), 1381 (s), 1219 (m), 1068 (m), 1026 (m), 810 (m), 428 (m) cm^{-1}.

Crystal Structure Determination. X-ray quality single crystals of **2**−**6** are obtained directly from the above preparations. All measurements were made on a Rigaku Mercury CCD X-ray diffractometer by using graphite monochromated Mo Kα (λ = 0.71070 Å). Each single crystal was mounted at the top of a glass fiber and cooled at 193 K in a stream of gaseous nitrogen. Cell parameters were refined by using the program CrystalClear (Rigaku and MSc, version 1.3, 2001) on all observed reflections. The collected data were reduced by using the program CrystalClear, and an absorption correction (multiscan) was applied, which resulted in transmission factors ranging from 0.401 to 0.539 for **2**, from 0.351 to 0.433 for **3**, from 0.308 to 0.810 for **4**, from 0.233 to 0.658 for **5**, and from 0.104 to 0.291 for **6**. The reflection data were also corrected for Lorentz and polarization effects.

The structures of **2**−**6** were solved by either direct methods[19] or heavy-atom Patterson methods[20a] and were expanded using Fourier techniques.[20b] For **2**, the orientation of each bridging cyanide group was found to be disordered, and the C and N atoms were refined with 50% probability of being C and N, i.e., C(7):N(1A) = 0.5:0.5 and N(1):C(7A) = 0.5:0.5. In addition, crystallographic analysis revealed particularly large voids within the crystal of **2**. Using the PLATON program[21] program, we estimated the void volume to be 821 Å^3 per unit cell, and there are approximately 40 non-hydrogen solvent atoms in the unit cell. Because of the dramatic loss of single-crystal character upon removal from the mother liquor and the small size of the crystal (0.25 × 0.10 × 0.08 mm^3), the absence of strong reflections at high angles did not permit satisfactory refinement of the solvent molecules, which led to a higher *R* value. For **5**, the crystal used may contain two Et_2O solvated molecules. However, numerous attempts to refine them failed, which resulted in large void (ca. 216 Å^3) within the crystal. In the case of **6**, we wish to note that the crystal used was weakly diffracting, especially at high angles, because of its rapid solvent loss upon removal from the mother liquor, which also led to a relatively high *R* value.

For compounds **2**−**6**, all non-hydrogen atoms, except for those from 4,4′-bipy (**5**) and Et_2O (**6**), were refined anisotropically. Hydrogen atoms for 4,4′-bipy (**5**) and Et_2O (**6**) were not located. All other hydrogen atoms were placed in geometrically idealized positions (C−H = 0.98 Å for methyl groups and C−H = 0.95 Å for phenyl groups) and constrained to ride on their parent atoms with $U_{iso}(H) = 1.2U_{eq}(C)$. All the calculations were performed on a Dell workstation using the CrystalStructure crystallographic software package (Rigaku/MSC, version 3.60, 2004). Important crystal and data collection parameters for **2**−**6** are summarized in Table 1.

Results and Discussion

Synthetic and Spectral Aspects. In the formation of the supramolecular cube $[((\eta^5\text{-}C_5Me_5)WS_3Cu_3)_8Cl_8(CN)_{12}Li_4]$,[17b] two findings were quite critical and intriguing. One is that 4 Li^+ and 8 Cl^- ions from the lithium chloride used were retained within the cube. The introduction of Li^+ or Cl^- ions into frameworks of the cube was considered to change its

(19) Sheldrick, G. M. *SHELXS-97, Program for X-ray Crystal Structure Solution*; University of Göettingen: Göettingen, Germany, 1997.

(20) (a) Beurskens, P. T.; Admiraal, G.; Beurskens, G.; Bosman, W. P.; Garcia-Granda, S.; Gould, R. O.; Smits, J. M. M.; Smykalla, C. *PATTY, The DIRDIF Program System*; Technical Report of the Crystallography Laboratory, University of Nijmegen: Nijmegen, The Netherlands, 1992. (b) Beurskens, P. T.; Admiraal, G.; Beurskens, G.; Bosman, W. P.; de Gelder, R.; Israel, R.; Smits, J. M. M. *DIRDIF99, The DIRDIF-99 Program System*; Technical Report of the Crystallography Laboratory, University of Nijmegen: Nijmegen, The Netherlands, 1999.

(21) Spek, A. J. *J. Appl. Crystallogr.* **2003**, *36*, 7.

Scheme 2

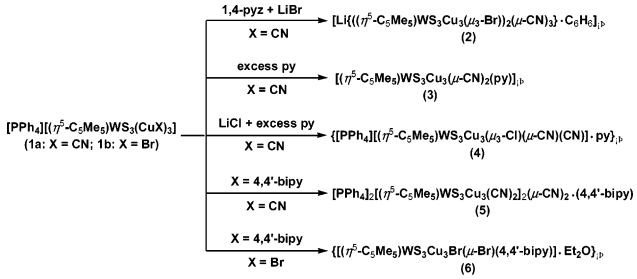

charge and thus enhance its solubility in solution. The other is that 1,4-pyz used removed part of cyanides but did not coordinate to any copper centers of **1a**. It is assumed that the combined utilization of nitrogen donor ligands (e.g., 1,4-pyz) and/or LiX (X = halides) may be a good approach to the construction of cluster-based supramolecular compounds. Therefore, we carried out an analogous reaction of **1a** with LiBr and 1,4-pyz in MeCN and an unusual 1D ladder-type chain polymer, $[Li\{((\eta^5\text{-}C_5Me_5)WS_3Cu_3(\mu_3{-}Br))_2(\mu\text{-}CN)_3\}\cdot C_6H_6]_\infty$ (**2**), was generated (Scheme 2). In this case, 1,4-pyz also did not bind at any copper centers but did remove part of the cyanides of **1a**. The Br^- ion from the LiBr used capped the void of the incomplete $[(\eta^5\text{-}C_5Me_5)WS_3Cu_3]$ cubane-like core, whereas the Li^+ ion acted as a counterion for the $\{((\eta^5\text{-}C_5Me_5)WS_3Cu_3(\mu_3\text{-}Br))_2(\mu\text{-}CN)_3\}^-$ anion. During the crystal growth of **2**, a large amount of red solid was observed to form, which may be ascribed to the low yield of **2**. The solid was virtually insoluble in common organic solvents; its identity could not be confirmed by elemental analysis, X-ray fluorescence analysis, or IR spectra, as the data for its C, H, and N analyses were always inconsistent and the IR spectra were quite messy. This unidentified resulting species, along with the different outcomes between **1a**/LiCl/1,4-pyz and **1a**/LiBr/1,4-pyz, implied that such an assembly system might proceed in a rather complicated way.

Because 1,4-pyz in the above reactions did not coordinate to any copper atom, we hoped that other strong donor ligands such as pyridine (py) could work at least partly on copper atoms and thus form other unique supramolecular frameworks. Therefore, we simply dissolved **1a** in excess py and a workup produced red prisms of 3D polymeric cluster $[(\eta^5\text{-}C_5Me_5)WS_3Cu_3(\mu\text{-}CN)_2(py)]_\infty$ (**3**) in 70% yield (Scheme 2). In this case, py served as both a solvent and a ligand, which replaced part of the cyanides and bound to one copper atom of **1a**.

Intriguingly, in a system of **1a**/LiCl with excess py, a similar workup to that used in the isolation of **3** formed a 1D chain polymeric cluster, $\{[PPh_4][(\eta^5\text{-}C_5Me_5)WS_3Cu_3Cl(\mu\text{-}CN)(CN)]\cdot py\}_\infty$ (**4**), as red platelets in 65% yield (Scheme 2). As mentioned later in this paper, the Cl^- ion capped the void of the incomplete $[(\eta^5\text{-}C_5Me_5)WS_3Cu_3]$ cubane-like core. The py molecule in this case worked somewhat differently. It did remove some cyanides of **1a** but did not coordinate at any Cu centers of **1a** and was included only as a crystal solvated molecule. This seems unusual because py has always been observed to coordinate at copper sites of cyanide-bridged clusters such as $[WOS_3Cu_3(CN)(py)_4]_\infty$, $\{[MoOS_3Cu_3(CN)(py)_3]\cdot 0.5C_6H_6\}_\infty$,[22] $[WS_4Cu_4(py)_4(\mu\text{-}CN)_2]_\infty$,[23] $[PPh_4]\text{-}\{[(\eta^5\text{-}C_5Me_5)WS_3Cu_2(CN)(py)]_2(\mu\text{-}CN)\}$,[24] and **3**.

Inspired by the above results, we naturally explored the reactions of **1a** with 4,4′-bipy to make 4,4′-bipy-linked supramolecular assemblies, because 4,4′-bipy is a versatile ditopic ligand, which has proven to be very useful in the formation of cluster-based supramolecular compounds.[3a,4d,17c] Surprisingly, a similar workup to that used in the isolation of **3** afforded $[PPh_4]_2[(\eta^5\text{-}C_5Me_5)WS_3Cu_3(CN)_2]_2(\mu\text{-}CN)_2\cdot$(4,4′-bipy) (**5**) in only 41% yield (Scheme 2), which was confirmed by elemental analysis, IR, and X-ray analysis to be the precursor **1a** crystallized with 1 equiv of 4,4′-bipy molecule. Again, the identity of the red-orange solid formed during the growth of the crystals of **5** was difficult to clearly characterize because of its quite low solubility in common organic solvents.

The failed assembly of **1a** with 4,4′-bipy prompted us to choose its bromine analogue, $[PPh_4][(\eta^5\text{-}C_5Me_5)WS_3(CuBr)_3]$ (**1b**). Fortunately, in this case, treatment of **1b** and 4,4′-bipy in DMF followed by a similar workup to that used in the isolation of **3** produced an interesting 2D cluster, $\{[(\eta^5\text{-}C_5Me_5)WS_3Cu_3Br(\mu\text{-}Br)(4,4'\text{-bipy})]\cdot Et_2O\}_\infty$ (**6**), as very thin red plates in 60% yield (Scheme 2). The different outcomes between this reaction and the previous reactions may be due to the fact that, relative to cyanide, bromide is more easily replaced by 4,4′-bipy.

Compounds **2**−**6** were relatively stable toward air and moisture. Compound **5** was slightly soluble in DMF and DMSO, whereas **2**−**4** and **6** were virtually insoluble in any common organic solvents, which excluded our further investigation of their physical and chemical properties in solution. The elemental analysis was consistent with the chemical formula of **2**−**6**. Relative to the terminal C≡N stretching vibration at 2129 cm^{-1} in the IR spectrum of **1a**, the bridging C≡N stretching vibrations of **2** and **3** shift to 2137 and 2152 cm^{-1}, respectively. Compounds **4** and **5** have one bridging C≡N and one terminal C≡N stretching vibration at 2160 and 2120 cm^{-1} (**4**) and 2154 and 2126 (**5**) cm^{-1}, respectively. In addition, the IR spectra of **2**−**6** show bridging W−S stretching vibrations at 439 (**2**), 469 and 424 (**3**), 445 and 430 (**4**), 428 (**5**), and 428 cm^{-1} (**6**), respectively.

Crystal Structure of $[Li\{((\eta^5\text{-}C_5Me_5)WS_3Cu_3(\mu_3\text{-}Br))_2(\mu\text{-}CN)_3\}\cdot C_6H_6]_\infty$ (2). Compound **2** crystallizes in the orthorhombic space group *Cmcm*, and the asymmetric unit contains one-quarter of the $[\{(\eta^5\text{-}C_5Me_5)WS_3Cu_3(\mu_3\text{-}Br)\}_2(\mu\text{-}CN)_3]^-$ anion, one-quarter of a Li^+ ion, and one-quarter of a solvated benzene molecule. As indicated by Figure 1, the $[(\eta^5\text{-}C_5Me_5)WS_3Cu_3(\mu_3\text{-}Br)]$ fragment may be viewed as having a distorted cubane-like structure in which one bromide fills into the void of the $[(\eta^5\text{-}C_5Me_5)WS_3Cu_3]$ incomplete cube of **1a** with three long Cu−Br distances (Table 2). The W(1), Cu(1), Br(1), S(2), C(1), and C(4) atoms are lying on the

(22) Jiao, C. M.; Qiao, S. B.; Xu, Q. F.; Lang, J. P. *Chin. J. Struct. Chem.* **2004**, *23*, 288.
(23) Lang, J. P.; Xu, Q. F.; Ji, W.; Elim, H. I.; Tatsumi, K. *Eur. J. Inorg. Chem*. **2004**, 86.
(24) Hou, H. W.; Zheng, H. G.; Ang, H. G.; Fan, Y.; Low, M. K. M.; Zhu, Y.; Wang, W. L.; Xin, X. Q.; Jiang, W.; Wong, W. T. *J. Chem. Soc., Dalton Trans.* **1999**, 2953.

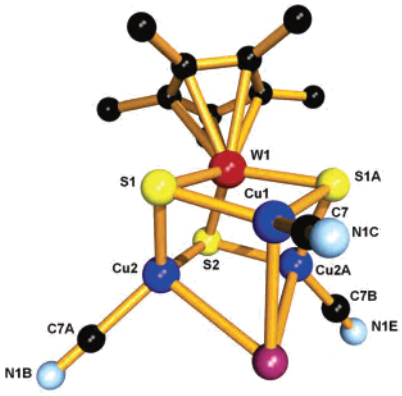

Figure 1. Perspective view of a $[(\eta^5\text{-}C_5Me_5)WS_3Cu_3(\mu_3\text{-}Br)(CN)_3]$ core of **2** with 50% thermal ellipsoids. Only one of the two orientations of each disordered cyanide is shown. All hydrogen atoms are omitted for clarity. Symmetry transformations used to generate equivalent atoms: A $x, y, -z + {}^3/_2$; B $x, -y, -z + 1$; C $-x, y, -z + {}^3/_2$.

Table 2. Selected Bond Lengths (Å) and Angles (deg) of **2**

W(1)···Cu(1)	2.661(4)	W(1)···Cu(2)	2.677(3)
W(1)···Cu(2A)	2.677(3)	W(1)−S(1)	2.284(6)
W(1)−S(1A)	2.284(6)	W(1)−S(2)	2.300(8)
Cu(1)−S(1)	2.236(7)	Cu(2)−S(2)	2.249(6)
S(2)−Cu(2A)	2.249(6)	Cu(1)−S(1A)	2.236(7)
Cu(2)−S(1)	2.264(7)	Cu(1)−Br(1)	2.887(7)
Cu(2)−Br(1)	2.788(5)	Br(1)−Cu(2A)	2.788(5)
Cu(1)−C(7)	1.91(3)	Cu(2)−C(7A)	1.907(19)
C(7)−N(1C)	1.12(5)	C(7A)-N(1B)	1.15(4)
S(1)−W(1)−S(1A)	105.1(3)	S(1)−W(1)−S(2)	106.09(19)
S(1A)−W(1)−S(2)	106.09(19)	Cu(1) ···W(1) ···Cu(2)	70.90(11)
Cu(1)···W(1) ···Cu(2A)	170.90(11)	Cu(2)···W(1) ···Cu(2A)	72.02(13)
C(7)−Cu(1)−S(1A)	121.7(3)	C(7)−Cu(1)−S(1)	121.7(3)
S(1)−Cu(1)−S(1A)	108.4(4)	C(7)−Cu(1)−Br(1)	99.8(8)
S(1A)−Cu(1)−Br(1)	99.4(2)	S(1)−Cu(1)−Br(1)	99.4(2)
C(7A)−Cu(2)−S(2)	128.1(7)	C(7A)−Cu(2)−S(1)	113.8(6)
S(2)−Cu(2)−S(1)	108.5(3)	C(7A)−Cu(2)−Br(1)	102.8(6)
S(2)−Cu(2)−Br(1)	96.62(19)	S(1)−Cu(2)−Br(1)	101.7(2)
Cu(2)−Br(1)−Cu(2A)	68.75(15)	Cu(2A)−Br(1)−Cu(1)	66.09(13)
Cu(2)−Br(1)−Cu(1)	66.09(13)	Cu(1)−S(1)−Cu(2)	86.9(3)
Cu(1)−S(1)−W(1)	72.1(2)	Cu(2)−S(1)−W(1)	72.11(19)
Cu(2)−S(2)−Cu(2A)	88.8(3)	Cu(2)−S(2)−W(1)	72.1(2)
Cu(2A)−S(2)−W(1)	72.1(2)	N(1B)−C(7A)−Cu(2)	176(2)
N(1C)−C(7)−Cu(1)	179.6(8)		

same crystallographic plane. The oxidation states of the tungsten and copper centers in **1a** (+6 and +1, respectively) are retained in **2**. The resulting $WS_3Cu_3(\mu_3\text{-}Br)$ cube is closely related to those observed in a neutral cluster, $\{WS_3Cu_3(\mu_3\text{-}Br)\}(PPh_3)_3S\cdot H_2O$,[25a] and a cationic cluster, $[(\eta^5\text{-}C_5Me_5)WS_3Cu_3(\mu_3\text{-}Br)(PPh_3)_3](PF_6)$.[25b] The three Cu atoms in **2** may be viewed as having a nearly trigonal planar coordination with a fourth weak Cu−Br interaction. The W(1)···Cu separations (2.661(4)−2.677(3) Å) are close to those observed in clusters containing trigonally coordinated Cu such as **1a** (2.668(2)−2.701(2) Å)[17b] and **1b** (2.649(1)−2.676(1) Å).[18a] The mean Cu−Br length of 2.821(7) Å is longer than that found in $\{WS_3Cu_3(\mu_3\text{-}Br)\}(PPh_3)_3S\cdot H_2O$ (2.761(1) Å) and $[(\eta^5\text{-}C_5Me_5)WS_3Cu_3(\mu_3\text{-}Br)(PPh_3)_3](PF_6)$ (2.713(1) Å). The mean Cu−μ_3-S bond length (2.249(7) Å) is comparable to those reported in other trigonally coordinated Cu clusters such as **1a** (2.242(5) Å) and **1b** (2.234(2) Å). The $[(\eta^5\text{-}C_5Me_5)WS_3]^-$ anion of **2** has a slightly distorted three-legged piano stool

(25) (a) Lang, J. P.; Zhu, H. Z.; Xin, X. Q.; Chen, M. Q.; Liu, K.; Zheng, P. J. *Chin. J. Chem.* **1993**, *11*, 21. (b) Yu, H.; Zhang, W. H.; Ren, Z. G.; Chen, J. X.; Wang, C. L.; Lang, J. P.; Elim, H. I.; Ji, W. *J. Organomet. Chem.* **2005**, *690*, 4027.

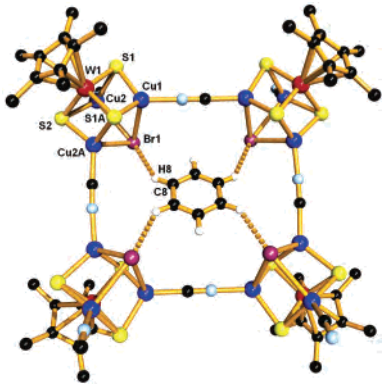

Figure 2. Perspective view of the repeating squarelike unit in **2**.

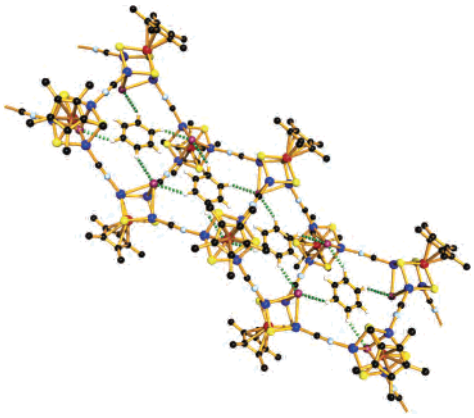

Figure 3. Perspective view of a portion of the 1D ladder-shaped chain of **2** extended along the *c* axis.

structure. The mean W−μ_3-S bond length (2.289(6) Å) is elongated by 0.02 Å compared with that of $[PPh_4][(\eta^5\text{-}C_5Me_5)WS_3]$ as a consequence of the coordination of S atoms to copper centers. The Cu−C/N and Cu−N/C distances of the bridging cyanide groups in **2** vary from 1.907(19) to 1.91(3) Å, which are close to those found in $[(\eta^5\text{-}C_5Me_5)WS_3Cu_2(PPh_3)(\mu\text{-}CN)]_2$ (Cu−N/C = 1.939(7) Å and Cu−C/N = 1.945(8) Å)[24] and $[Cu(4\text{-}CNpy)(\mu\text{-}CN)]_\infty$ (Cu−N/C = 1.907(2) Å and Cu−C/N = 1.999(2) Å).[26] The Cu−C/N−N/C angles are in the range 176(2)−179.6(8)°.

Interestingly, four $[(\eta^5\text{-}C_5Me_5)WS_3Cu_3(\mu_3\text{-}Br)]$ fragments in **2** are linked via four cyanide bridges, forming a repeating squarelike $[\{(\eta^5\text{-}C_5Me_5)WS_3Cu_3(\mu_3\text{-}Br)(\mu\text{-}CN)\}_4](\mu\text{-}CN)_2^{2-}$ unit with a crystallographic C_{2v} symmetry (Figure 2). Each squarelike unit is further interconnected by another four cyanides to form a 1D ladder-shaped anionic chain extending along the crystallographic *c* axis (Figure 3). The Cu−μ-CN−Cu portions are almost linear. Alternatively, the $[(\eta^5\text{-}C_5Me_5)WS_3Cu_3(\mu_3\text{-}Br)]$ fragment in **2** may be topologically considered as being a three-connecting node (b), which is linked to three equivalent nodes via Cu−μ-CN−Cu bridges to form this 1D chain polymer. The average chain-to-chain separation is ca. 10.4 Å, with the $[\{(\eta^5\text{-}C_5Me_5)WS_3Cu_3(\mu_3\text{-}Br)\}_4(\mu\text{-}CN)_6]_n^{2n-}$ anionic layers separated by η^5-C_5Me_5 groups. It is difficult to unambiguously identify lithium ions in a crystal structure, particularly in a unit cell that contains so many heavy atoms, and the peak located in the 4-fold

(26) Kappenstein, C.; Hugel, R. P. *Inorg. Chem.* **1977**, *16*, 250.

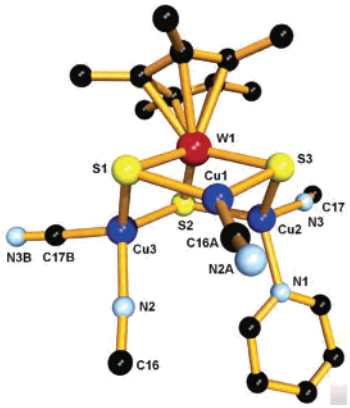

Figure 4. Perspective view of a repeating unit of **3** with 50% probability level thermal ellipsoids. All hydrogen atoms are omitted for clarity. Symmetry transformations used to generate equivalent atoms: A $x - {}^1/_2$, $-y + {}^3/_2$, $-z + 2$; B $-x + 1$, $y - {}^1/_2$, $-z + {}^3/_2$.

Table 3. Selected Bond Lengths (Å) and Angles (deg) of **3**

W(1)−S(2)	2.256(2)	W(1)−S(1)	2.272(2)
W(1)−S(3)	2.283(2)	W(1)···Cu(1)	2.6497(12)
W(1)···Cu(2)	2.7421(12)	W(1)···Cu(3)	2.7599(11)
Cu(1)−C(16A)	1.889(10)	Cu(1)−S(3)	2.213(3)
Cu(1)−S(1)	2.217(3)	Cu(2)−N(3)	2.024(9)
Cu(2)−N(1)	2.070(8)	Cu(2)−S(3)	2.267(3)
Cu(2)−S(2)	2.281(2)	Cu(3)−C(17B)	1.962(9)
Cu(3)−N(2)	2.046(8)	Cu(3)−S(1)	2.283(3)
Cu(3)−S(2)	2.287(2)	N(2)−C(16)	1.140(12)
N(3)−C(17)	1.148(12)		
S(2)−W(1)−S(1)	105.99(8)	S(2)−W(1)−S(3)	105.73(8)
S(1)−W(1)−S(3)	105.40(9)	Cu(1)···W(1)···Cu(2)	82.63(4)
Cu(1)···W(1)···Cu(3)	80.14(4)	Cu(2)···W(1)···Cu(3)	85.73(4)
C(16A)−Cu(1)−S(3)	127.6(3)	C(16A)−Cu(1)−S(1)	121.3(3)
S(3)−Cu(1)−S(1)	109.72(10)	N(3)−Cu(2)−N(1)	95.1(3)
N(3)−Cu(2)−S(3)	114.2(2)	N(1)−Cu(2)−S(3)	117.8(2)
N(3)−Cu(2)−S(2)	109.6(3)	N(1)−Cu(2)−S(2)	114.7(2)
S(3)−Cu(2)−S(2)	105.42(9)	C(17B)-Cu(3)−N(2)	101.2(4)
C(17B)−Cu(3)−S(1)	113.1(3)	N(2)−Cu(3)−S(1)	104.5(2)
C(17B)−Cu(3)−S(2)	115.6(3)	N(2)−Cu(3)−S(2)	117.6(2)
S(1)−Cu(3)−S(2)	104.60(9)	Cu(1)−S(1)−W(1)	72.34(7)
Cu(1)−S(1)−Cu(3)	101.42(10)	W(1)−S(1)−Cu(3)	74.60(7)
W(1)−S(2)−Cu(2)	74.36(7)	W(1)−S(2)−Cu(3)	74.81(7)
Cu(2)−S(2)−Cu(3)	110.04(10)	Cu(1)−S(3)−Cu(2)	105.25(10)
Cu(1)−S(3)−W(1)	72.21(8)	Cu(2)−S(3)−W(1)	74.12(8)
Cu(1)−C(16A)-N(2A)	172.4(9)	C(16A)−N(2A)−Cu(3A)	168.4(8)
Cu(2)−N(3)−C(17)	164.1(9)	N(3)−C(17)−Cu(3D)	168.1(9)

axis was identified as being attributable to lithium ions. In addition, a solvated benzene molecule lies at the center of each squarelike unit; its four hydrogen atoms interact with four Br atoms of the squarelike unit to symmetrically form four C−H···Br (3.54(4) Å, 140.8°) hydrogen bonds, which may stabilize the whole ladder-shaped chain framework.

Crystal Structure of $[(\eta^5\text{-}C_5Me_5)WS_3Cu_3(\mu\text{-}CN)_2(py)]_\infty$ (3). Compound **3** crystallizes in orthorhombic space group $P2_12_12_1$, and the asymmetric unit contains one discrete molecule of $[(\eta^5\text{-}C_5Me_5)WS_3Cu_3(\mu\text{-}CN)_2(py)]$. Figure 4 shows the perspective view of the repeating unit of **3**, and Table 3 lists selected bond lengths and angles for **3**. The tungsten and copper centers in **3** again kept their +6 and +1 oxidation states in **1a**. Although the repeating unit $[(\eta^5\text{-}C_5Me_5)WS_3Cu_3(\mu\text{-}CN)_2(py)]$ assumes an incomplete cubane-like $[(\eta^5\text{-}C_5Me_5)WS_3Cu_3]$ core structure similar to that of **1a**, its three Cu centers have different coordination environments. Cu(1) remains in a trigonal planar coordination geometry, whereas Cu(2) (or Cu(3)) is tetrahedrally bound by two μ_3-S and two C atoms (or one N(py), one C, and

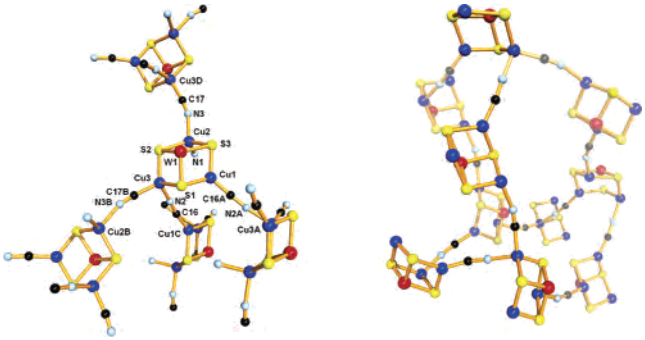

Figure 5. (a) Perspective view of the interactions of a central $[(\eta^5\text{-}C_5Me_5)WS_3Cu_3]$ core via four CN bridges in **3** (left). Symmetry transformations used to generate equivalent atoms: A $x - {}^1/_2$, $-y + {}^3/_2$, $-z + 2$; B $-x + 1$, $y - {}^1/_2$, $-z + {}^3/_2$; C $x + {}^1/_2$, $-y + {}^3/_2$, $-z + 2$; D $-x + 1$, $y + {}^1/_2$, $-z + {}^3/_2$. (b) Adamantane type unit within the network of **3** (right). The η^5-C_5Me_5 and pyridyl groups are omitted for clarity.

two μ_3-S atoms). Because of the change in the coordination geometries of the three copper atoms, the W···Cu contacts are also different: W(1)···Cu(1) = 2.6497(12) Å, W(1)···Cu(2) = 2.7421(12) Å, and W(1)···Cu(3) = 2.7599(11) Å, which correlate with the number of bonding interactions at Cu centers. The shorter W(1)···Cu(1) contact is comparable to those observed in **1a** and **2**, whereas the longer ones (W(1)···Cu(2) and W(1)···Cu(3)) are close to those in clusters containing tetrahedrally coordinated Cu, such as $[(\eta^5\text{-}C_5Me_5)WS_3Cu]_4$ (2.742(3)−2.761(3) Å)[27a] and $[WS_4Cu_4(dppm)_4](PF_6)_2$ (2.764(1)−2.755(1) Å).[27b] It is noted that the mean bond angle of Cu···W(1)···Cu in **3** is 82.83(4)°, almost 10° larger than that of **1a**. The Cu−μ_3-S bond lengths also reflect the mode of coordination of copper atoms: an average of 2.215(3) Å for a trigonal geometry and an average of 2.280(3) Å for a tetrahedral environment. We assigned the atom coordinated at Cu(1) or Cu(3) to carbon and that bound to Cu(2) or Cu(3) to nitrogen, on the basis of peak heights on the Fourier map and bond lengths. The mean Cu−C and Cu−N distances of the bridging cyanide groups are 1.926(9) and 2.035(8) Å, respectively, which are close to those found in $KCu(CN)_2$ (Cu−C/Cu−N = 1.919(3)/2.052 Å)[28a] and $Na[Cu(CN)_2]\cdot 2H_2O$ (Cu−C/Cu−N = 1.903(8)/1.992(8 Å).[28b] However, the possibility of a partial disorder of atoms arising from the opposite orientation of cyanide cannot be ruled out in the structure of **3**.

As shown in Figure 5a, the repeating unit $[(\eta^5\text{-}C_5Me_5)WS_3Cu_3(\mu\text{-}CN)_2(py)]$ is coordinated by four bridging cyanide groups, which link four crystallographically equivalent clusters that lie at the corners of a very distorted tetrahedron. From a topological perspective, each cluster $[(\eta^5\text{-}C_5Me_5)WS_3Cu_3]$ core serves as a tetrahedral node (c), to form a single adamantine type unit (Figure 5b), which is interconnected via μ-CN anions to form a 3D network (Figure 6). Such a 3D structure is unprecedented in thiometalate chemistry. It should be noted that the pyridyl groups coordinated at Cu(2) centers and the bulky η^5-C_5Me_5 groups on W(1) atoms

(27) (a) Lang, J. P.; Kawaguchi, H.; Tatsumi, K. *J. Organomet. Chem.* **1998**, *509*, 109. (b) Lang, J. P.; Tatsumi, K. *Inorg. Chem.* **1998**, *37*, 6308.
(28) (a) Cromer, D. T. *J. Phys. Chem.* **1957**, *61*, 1388. (b) Kappenstein, C.; Hugel, R. P. *Inorg. Chem.* **1977**, *16*, 250.

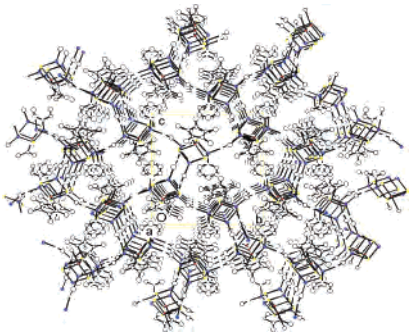

Figure 6. Unit-cell packing diagram of **3** looking down the *a* axis. All hydrogen atoms are omitted for clarity.

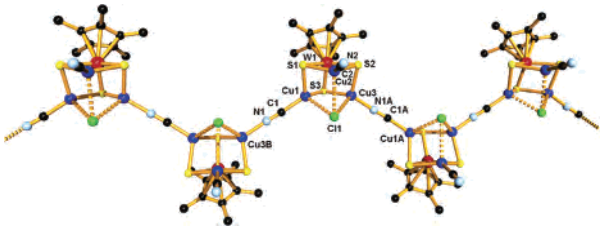

Figure 7. Perspective view of a portion of the 1D zigzag chain (extended along the *c* axis) of **4**. All hydrogen atoms are omitted for clarity. Symmetry transformations used to generate equivalent atoms: A $x, -y + {}^3/_2, z - {}^1/_2$; B $-x, -y + {}^3/_2, z + {}^1/_2$.

occupy the resulting adamantine cavities, thereby preventing interpenetration of networks. The Cu−μ-CN−Cu bridges in **3** are somewhat bent, with Cu(1)−C(16A)−N(2A), C(16A)−N(2A)−Cu(3A), Cu(2)−N(3)−C(17), and N(3)−C(17)−Cu(3D) angles of 172.4(9), 168.4(8), 164.1(9), and 168.1(9)°, respectively. This is probably due to the demand of the formation of the diamond-related framework in **3**.

Crystal Structure of {[PPh$_4$][(η^5-C$_5$Me$_5$)WS$_3$Cu$_3$(μ_3-Cl)(CN)(μ-CN)]·py}$_\infty$ (4). Compound **4** crystallizes in the monoclinic space group $P2_1/c$, and the asymmetric unit contains one discrete [(η^5-C$_5$Me$_5$)WS$_3$Cu$_3$(μ_3-Cl)(CN)(μ-CN)]$^-$ anion, one [PPh$_4$]$^+$ cation, and one solvated pyridine molecule. An X-ray analysis revealed that **4** has a one-dimensional zigzag anionic chain, which is composed of the repeating [(η^5-C$_5$Me$_5$)WS$_3$Cu$_3$(μ_3−Cl)(CN)] units and is stacked along the crystallographic *c* axis via Cu−μ-CN−Cu bridges (Figure 7). The anionic chains are separated by [PPh$_4$]$^+$ cations and pyridine solvent molecules, and no hydrogen bonding interaction exists among the chain and the phenyl or pyridine hydrogens. Topologically, the [(η^5-C$_5$Me$_5$)WS$_3$Cu$_3$] core in **4** acts as a two-connecting node (d). The [(η^5-C$_5$Me$_5$)WS$_3$Cu$_3$(μ_3-Cl)(CN)] unit may be viewed as having a severely distorted cubane-like structure in which one chloride fills into the void of the incomplete cube of **1a** with one long and two short Cu−Cl distances (Cu(1)−Cl(1) = 2.648(4), Cu(2)−Cl(1) = 2.952(8), Cu(3)−Cl(1) = 2.613(4) Å) (Table 4). The resulting [(η^5-C$_5$Me$_5$)WS$_3$Cu$_3$(μ_3-Cl)] cube is closely related to those of neutral clusters [WES$_3$Cu$_3$(PPh$_3$)$_3$(μ_3-Cl)] (E = O, S).[29] The three Cu atoms in **4** are not equivalent and their coordination variability ranges from a strongly distorted tetrahedron (Cu(1) and Cu(3)) to a nearly trigonal planar coordination (Cu(2)) with a long Cu(2)−Cl(1) interaction. Because of the different coordination geometries of the copper atoms, the W(1)···Cu(2) separation (2.679(2) Å) is somewhat shorter than the mean value of the W(1)···Cu(1) and W(1)···Cu(3) separations (2.698(2) Å). The various Cu−μ_3-S bond lengths show the different coordination modes of the three copper atoms in **4**: an average of 2.240(5) Å for a trigonal geometry and an average of 2.271(5) Å for a tetrahedral environment. The mean Cu−Cl length of 2.738(4) Å is ca. 0.1 Å longer than those observed in [WES$_3$Cu$_3$(PPh$_3$)$_3$(μ_3-Cl)] (E = O, S) (Cu−Cl = 2.635(2) Å). The Cu−μ-CN−Cu portions in **4** are almost linear, with the Cu(1)−N(1)−C(1) and N(1)−C(1)−Cu(3B) angles being close to 180°. Again, we assigned the atom coordinated at Cu(3) to carbon and that bound to Cu(1) to nitrogen, on the basis of peak heights on the Fourier map and bond lengths. The Cu(1)−C(1) and Cu(3)−N(1A) distances of the bridging cyanide groups in **4,** 1.868(14) and 1.947(17) Å, are slightly shorter than those of the corresponding ones in **3**.

Table 4. Selected Bond Lengths (Å) and Angles (deg) of **4**

W(1)−S(1)	2.265(4)	W(1)−S(3)	2.277(4)
W(1)−S(2)	2.277(4)	W(1)···Cu(2)	2.679(2)
W(1)···Cu(1)	2.697(2)	W(1)···Cu(3)	2.699(2)
Cu(1)−C(1)	1.868(14)	Cu(1)−S(3)	2.265(4)
Cu(1)−S(1)	2.268(5)	Cu(1)−Cl(1)	2.648(4)
Cu(2)−C(2)	1.943(2)	Cu(2)−S(1)	2.239(5)
Cu(2)−S(2)	2.241(5)	Cu(3)−N(1A)	1.947(17)
Cu(3)−S(2)	2.267(4)	Cu(3)−S(3)	2.282(4)
Cu(3)−Cl(1)	2.613(4)	Cu(2)−Cl(1)	2.952(8)
C(1)−N(1)	1.138(19)	C(2)−N(2)	1.08(2)
S(1)−W(1)−S(3)	105.82(15)	S(1)−W(1)−S(2)	105.64(15)
S(3)−W(1)−S(2)	106.47(14)	Cu(1)···W(1)···Cu(2)	71.87(7)
Cu(2)···W(1)···Cu(3)	72.92(7)	Cu(1)···W(1)···Cu(3)	70.39(6)
C(1)−Cu(1)−S(3)	126.0(5)	C(1)−Cu(1)−S(1)	114.4(5)
S(3)−Cu(1)−S(1)	106.11(16)	C(1)−Cu(1)−Cl(1)	106.6(5)
S(3)−Cu(1)−Cl(1)	96.47(14)	S(1)−Cu(1)−Cl(1)	103.60(16)
C(2)−Cu(2)−S(1)	122.3(6)	C(2)−Cu(2)−S(2)	122.3(6)
S(1)−Cu(2)−S(2)	107.77(16)	N(1A)−Cu(3)−S(2)	115.0(5)
N(1A)−Cu(3)−S(3)	125.7(4)	S(2)−Cu(3)−S(3)	106.63(15)
N(1A)−Cu(3)−Cl(1)	106.5(5)	S(2)−Cu(3)−Cl(1)	101.80(15)
S(3)−Cu(3)−Cl(1)	97.03(14)	Cu(2)−S(1)−W(1)	72.98(13)
Cu(2)−S(1)−Cu(1)	88.84(16)	W(1)−S(1)−Cu(1)	73.02(12)
Cu(2)−S(2)−Cu(3)	90.28(16)	Cu(2)−S(2)−W(1)	72.72(13)
Cu(3)−S(2)−W(1)	72.87(12)	Cu(1)−S(3)−W(1)	72.86(12)
Cu(1)−S(3)−Cu(3)	86.32(15)	W(1)−S(3)−Cu(3)	72.61(12)
Cu(3)−Cl(1)−Cu(1)	72.47(10)	N(1)−C(1)−Cu(1)	177.0(15)
N(2)−C(2)−Cu(2)	178(2)	C(1)−N(1)−Cu(3B)	175.6(14)

Crystal Structure of [PPh$_4$]$_2$[(η^5-C$_5$Me$_5$)WS$_3$Cu$_3$(CN)$_2$]$_2$-(μ-CN)$_2$·(4,4′-bipy) (5). Crystal **5** crystallizes in the triclinic space group $P\bar{1}$, and the asymmetric unit consists of one-half of a {[(η^5-C$_5$Me$_5$)WS$_3$Cu$_3$(CN)$_2$]$_2$(μ-CN)$_2$}$^{2-}$ dianion, one [PPh$_4$]$^+$ cation, and one 4,4′-bipy molecule. Figure 8 shows the perspective view of the dianion of **5**, and Table 5 lists selected bond lengths and angles. Compound **5** consists of two [(η^5-C$_5$Me$_5$)WS$_3$Cu$_3$(CN)$_3$]$^-$ anions that are bridged via a pair of Cu−μ-CN−Cu bridges, forming a double, incomplete cubane-like structure with a crystallographic center of inversion lying at the center of the W(1) and W(1A) line. Topologically, each [(η^5-C$_5$Me$_5$)WS$_3$Cu$_3$] core in **5** acts a mono-connecting node (node (e) in Scheme 1). The structure is closely related to that of **1a** with some differences. In **1a**, the two [(η^5-C$_5$Me$_5$)WS$_3$Cu$_3$(CN)$_3$]$^-$ anions are weakly bridged via pairs of Cu−μ-CN−Cu bridges (Cu−C/N =

(29) Müller, A.; Bögge, H.; Schimanski, U. *Inorg. Chim. Acta* **1983**, *69*, 5.

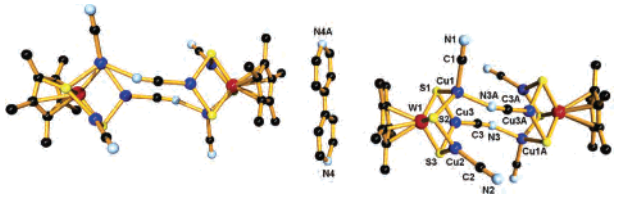

Figure 8. Perspective view of the $\{[(\eta^5\text{-}C_5Me_5)WS_3Cu_3(CN)_2]_2(\mu\text{-}CN)_2\}^{2-}$ dianions along with the sandwiched 4,4′-bipy molecule in **5**. All hydrogen atoms are omitted for clarity. Symmetry transformations used to generate equivalent atoms: A $-x+2, -y+1, -z+1$.

Table 5. Selected Bond Lengths (Å) and Angles (°) of **5**

W(1)−S(2)	2.266(2)	W(1)−S(1)	2.269(2)
W(1)−S(3)	2.293(2)	W(1)···Cu(2)	2.6562(14)
W(1)···Cu(3)	2.6714(13)	W(1)···Cu(1)	2.7683(15)
Cu(1)−C(1)	1.930(10)	Cu(1)−N(3A)	2.111(8)
Cu(1)−S(2)	2.277(3)	Cu(1)−S(1)	2.319(3)
Cu(2)−C(2)	1.868(11)	Cu(2)−S(2)	2.219(3)
Cu(2)−S(3)	2.233(3)	Cu(3)−C(3)	1.884(9)
Cu(3)−S(1)	2.229(3)	Cu(3)−S(3)	2.233(3)
N(3)−Cu(1A)	2.111(8)	C(1)−N(1)	1.133(4)
C(2)−N(2)	1.163(15)	C(3)−N(3)	1.155(12)
S(2)−W(1)−S(1)	104.73(9)	S(2)−W(1)−S(3)	105.58(9)
S(1)−W(1)−S(3)	105.61(9)	Cu(2)···W(1)···Cu(3)	76.72(5)
Cu(2)···W(1)···Cu(1)	69.25(4)	Cu(3)···W(1)···Cu(1)	72.68(5)
C(1)−Cu(1)−N(3A)	111.2(4)	C(1)−Cu(1)−S(2)	110.2(3)
N(3A)−Cu(1)−S(2)	113.6(3)	C(1)−Cu(1)−S(1)	116.3(3)
N(3A)−Cu(1)−S(1)	102.4(2)	S(2)−Cu(1)−S(1)	102.80(10)
C(2)−Cu(2)−S(2)	120.4(4)	C(2)−Cu(2)−S(3)	129.7(4)
S(2)−Cu(2)−S(3)	109.24(10)	C(3)−Cu(3)−S(1)	126.9(3)
C(3)−Cu(3)−S(3)	123.9(3)	S(1)−Cu(3)−S(3)	109.09(9)
Cu(3)−S(1)−W(1)	72.87(8)	Cu(3)−S(1)−Cu(1)	90.31(9)
W(1)−S(1)−Cu(1)	74.22(8)	Cu(2)−S(2)−W(1)	72.63(8)
Cu(2)−S(2)−Cu(1)	86.59(9)	W(1)−S(2)−Cu(1)	75.09(8)
Cu(3)−S(3)−Cu(2)	95.50(11)	Cu(3)−S(3)−W(1)	72.34(8)
Cu(2)−S(3)−W(1)	71.85(8)	N(1)−C(1)−Cu(1)	177.8(10)
N(2)−C(2)−Cu(2)	176.2(12)	C(3A)−N(3A)−Cu(1)	155.1(8)
N(3)−C(3)−Cu(3)	171.7(9)		

2.44(3) Å); the two Cu centers are trigonal planar, whereas the third one is pseudo-tetrahedral. In **5**, the two cluster anions are tightly connected by the two Cu−μ-CN−Cu bridges, as the Cu(3)−C(3) or Cu(1A)−N(3) bond lengths are much shorter, amounting to 1.884(9) and 2.111(8) Å, respectively. Thus, Cu(1) adopts a distorted tetrahedral geometry, with bond angles of 102.4(2)−116.3(3)° around Cu(1). The W(1)···Cu contacts of **5** change accordingly: W(1)···Cu(1) = 2.7683(15) Å, W(1)···Cu(2) = 2.6557(14) Å, and W(1)···Cu(3) = 2.6715(13) Å. The long W(1)···Cu(1) contact is close to those of the corresponding ones of **3**, whereas the two short W(1)···Cu ones are similar to those of the corresponding ones of **1a** and **2**−**4**. The Cu−μ_3-S and terminal Cu−C lengths are normal compared to those of the corresponding ones in **1a** and **2**−**4**. Interestingly, the 4,4′-bipy molecule in the crystal of **5** does not coordinate at copper centers but is sandwiched between the two cluster dianions with evident $\pi-\pi$ interactions (3.616(14) Å) between each pyridyl group and its nearest η^5-C_5Me_5 group, thereby affording chains of cluster dianion/4,4′-bipy units running along the *c* axis (see the Supporting Information).

Crystal Structure of $\{[(\eta^5\text{-}C_5Me_5)WS_3Cu_3Br(\mu\text{-}Br)(4,4'\text{-bpy})]\cdot Et_2O\}_\infty$ (6). Compound **6** crystallizes in orthorhombic space group *Pbcn*, and the asymmetric unit contains a neutral molecule, $[(\eta^5\text{-}C_5Me_5)WS_3Cu_3Br(\mu\text{-}Br)(4,4'\text{-bpy})]$, and a solvated Et_2O molecule. An X-ray analysis revealed that **6**

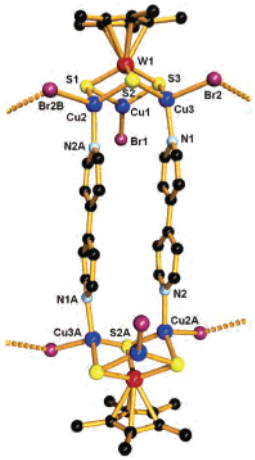

Figure 9. Perspective view of the repeating unit of **6**. All hydrogen atoms and Et_2O solvated molecules are omitted for clarity. Symmetry transformations used to generate equivalent atoms: A $-x, -y+1, -z+1$; B $-x+{}^1/_2, y+{}^1/_2, z$.

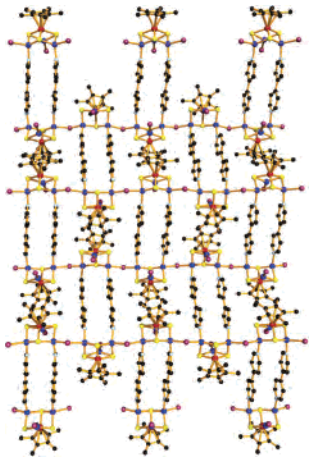

Figure 10. Extended structure of **6** looking down the *c* axis. All hydrogen atoms and Et_2O solvated molecules are omitted for clarity.

consists of repeating dimeric $[(\eta^5\text{-}C_5Me_5)WS_3Cu_3Br(4,4'\text{-bpy})]_2$ units (Figure 9), which are further interconnected by four Cu−μ-Br−Cu bridges to form a 2D brick-wall layer extending along the *ab* plane (Figure 10). The layers are squeezed with Et_2O solvent molecules (see the Supporting Information), and no evident interactions between layers and the Et_2O molecules exist. Each brick-like cavity is estimated to have dimensions of 11.2 Å × 11.5 Å and is occupied by two $[(\eta^5\text{-}C_5Me_5)WS_3Cu_3Br]$ fragments from two other dimers. Each dimer is centrosymmetrically related and consists of two $[(\eta^5\text{-}C_5Me_5)WS_3Cu_3Br]$ fragments connected by a pair of parallel 4,4′-bpy bridges. The resulting narrow mesh is estimated to have a size of 3.5 Å × 11.2 Å. The core structure of each $[(\eta^5\text{-}C_5Me_5)WS_3Cu_3Br]$ fragment closely resembles that of **1b**. Of the three copper atoms, Cu(1) is three-coordinated by one terminal Br and two μ_3-S atoms and the W(1)···Cu(1) contact is relatively short (2.625(3) Å) (Table 6). On the other hand, Cu(2) and Cu(3) are tetrahedrally coordinated by a N atom (4,4′-bipy), a μ-Br atom, and two μ_3-S atoms and the W(1)···Cu interactions are slightly weaker (2.697(3) and 2.705(3) Å). Topologically, each $[(\eta^5\text{-}C_5Me_5)WS_3Cu_3]$ core in **6** serves as a three-connecting node (node f in Scheme 1). The $[(\eta^5\text{-}C_5Me_5)WS_3$-

Table 6. Selected Bond Lengths (Å) and Angles (deg) of **6**

W(1)−S(2	2.272(5)	W(1)−S(3)	2.284(5)
W(1)−S(1)	2.284(6)	W(1)···Cu(1)	2.625(3)
W(1)···Cu(2)	2.697(3)	W(1)···Cu(3)	2.705(3)
Cu(1)−S(1)	2.209(7)	Cu(1)−S(3)	2.217(6)
Cu(1)−Br(1)	2.279(4)	Cu(2)−N(2A)	1.998(17)
Cu(2)−S(1)	2.240(6)	Cu(2)−S(2)	2.242(6)
Cu(2)−Br(2B)	2.501(4)	Cu(3)−N(1)	2.030(15)
Cu(3)−S(3)	2.242(6)	Cu(3)−S(2)	2.250(6)
Cu(3)−Br(2)	2.516(4)	N(2)−Cu(2A)	1.998(17)
S(2)−W(1)−S(3)	105.40(19)	S(2)−W(1)−S(1)	105.5(2)
S(3)−W(1)−S(1)	105.6(2)	Cu(1)···W(1)···Cu(2)	77.52(9)
Cu(1)···W(1)···Cu(3)	75.72(9)	Cu(2)···W(1)···Cu(3)	80.38(8)
S(1)−Cu(1)−S(3)	110.6(2)	S(1)−Cu(1)−Br(1)	123.8(2)
S(3)−Cu(1)−Br(1)	125.5(2)	N(2A)−Cu(2)−S(1)	117.5(6)
N(2A)−Cu(2)−S(2)	112.6(6)	S(1)−Cu(2)−S(2)	108.0(2)
N(2A)−Cu(2)−Br(2B)	103.2(6)	S(1)−Cu(2)−Br(2B)	109.8(2)
S(2)−Cu(2)−Br(2B)	104.85(18)	N(1)−Cu(3)−S(3)	118.8(6)
N(1)−Cu(3)−S(2)	115.7(5)	S(3)−Cu(3)−S(2)	107.6(2)
N(1)−Cu(3)−Br(2)	99.6(5)	S(3)−Cu(3)−Br(2)	109.66(18)
S(2)−Cu(3)−Br(2)	104.10(19)	Cu(2C)−r(2)−Cu(3)	106.38(13)
Cu(1)−S(1)−Cu(2)	97.0(2)	Cu(1)−S(1)−W(1)	71.5(2)
Cu(2)−S(1)−W(1)	73.18(19)	Cu(2)−S(2)−Cu(3)	101.8(2)
Cu(2)−S(2)−W(1)	73.36(17)	Cu(3)−S(2)−W(1)	73.47(16)
Cu(1)−S(3)−Cu(3)	94.4(2)	Cu(1)−S(3)−W(1)	71.35(17)
Cu(3)−S(3)−W(1)	73.41(17)		

Cu_3Br] fragments are interconnected by μ-Br at Cu(3) and Cu(2B), forming 1D zigzag chains extending along the *b* axis, where the orientation of the [(η^5-C_5Me_5)WS_3Cu_3Br] fragment is alternating. Alternatively, the 2D brick-wall layer structure of **6** can be viewed as being built of [(η^5-C_5Me_5)WS_3Cu_3Br(μ-Br)] chains linked by pairs of parallel 4,4′-bpy bridges along the *a* axis. Within the chain, the Cu(3)−Br(2)−Cu(2C) ($-x + {}^1/_2$, $y - {}^1/_2$, *z*) bond angle is 106.4(2)° and the two bond lengths (Cu(3)−μ-Br(2), 2.516(4) Å; Cu(2C)−μ-Br(2), 2.501(4) Å) are slightly longer than those of $[Et_4N]_2[Cu_2Br_4]$ (2.448 Å)[30a] and $[Pr^n{}_4N]_4[Cu_4Br_6]$ (2.398 Å).[30b] The average Cu−μ_3-S and Cu−N (4,4′-bipy) distances are normal.

Conclusions

The construction of interesting polydimensional supramolecular arrays **2**−**6** from reactions of the preformed cluster **1a** or **1b** with 1,4-pyz, py, and 4,4′-bipy has been investigated. In these compounds, the [(η^5-C_5Me_5)WS_3Cu_3] cluster core was retained and served as multiconnecting nodes for producing unique topological [(η^5-C_5Me_5)WS_3Cu_3]-based architectures. Compound **2** displays a 1D ladder-shaped chain of squarelike $\{[(\eta^5\text{-}C_5Me_5)WS_3Cu_3Br(\mu\text{-}CN)]_4\}(\mu\text{-}CN)_2^{2-}$ anions linked by Cu−μ-CN−Cu bridges. Compound **3** consists of a single diamondlike 3D network in which each incomplete cubane-like (η^5-C_5Me_5)WS_3Cu_3 unit, serving as a tetrahedral node, interconnects with four other nearby units by Cu−μ-CN−Cu bridges. This structure, along with the existence of such a tetrahedral node, is rare in the cluster-based supramolecular compounds. Compound **4** contains a 1D zigzag chain structure made of the cubane-like [(η^5-C_5Me_5)WS_3Cu_3Cl(μ-CN)(CN)]$^-$ anions linked by Cu−μ-CN−Cu bridges. Compound **5** contains a dimeric structure in which the two incomplete cubane-like [(η^5-C_5Me_5)WS_3-$(CuCN)_2$(μ-CN)]$^-$ anions are strongly held together via a pair of Cu−μ-CN−Cu bridges and $\pi-\pi$ interactions between each pyridyl group of 4,4′-bipy and its nearest η^5-C_5Me_5 group. Compound **6** contains a neutral 2D brick-wall layer structure in which dimers of [(η^5-C_5Me_5)WS_3Cu_3Br(4,4′-bipy)]$_2$ are linked via four Cu−μ-Br−Cu bridges. These interesting structures, along with the supramolecular cube reported previously[17b] make **1a** or **1b** very promising precursors for the rational design and construction of cluster-based supramolecular compounds. We are currently extending this work by investigating the assembly of new [(η^5-C_5Me_5)WS_3Cu_3]-based networks from reactions of **1a** or **1b** with other multitopic ligands such as 2,4,6-tri-4-pyridyl-1,3,5-triazine and 5,10-15,20-tetra(4-pyridyl)-21H,23H-porphine.

Acknowledgment. This work was supported by the Distinguished Young Scholar Fund of NNSF to J.P.L. (20525101), the NSF of Jiangsu Province (BK2004205), the Specialized Research Fund for the Doctoral Program of Higher Education (20050285004), and the State Key Laboratory of Coordination Chemistry, Nanjing University, China. The authers appreciate the useful suggestions of the reviewers.

Supporting Information Available: Crystallographic data of compounds **2**−**6** (cif) and cell packing diagrams of **2** and **4**−**6** (pdf). This material is available free of charge via the Internet at http://pubs.acs.org.

IC060115P

(30) (a) Asplund, M.; Jagner, S. *Acta Chem. Scand*. **1984**, *13*, 5. (b) Asplund, M.; Jagner, S. *Acta Chem*. *Scand*. **1984**, *72*, 5.